RSC Advances




ROYAL SOCIETY OF CHEMISTRY

www.rsc.org/advances

RSC Advances

ARTICLE

# Facile Synthesis of Silver Submicrospheres and Their Applications

Bin Tang,[a,b] Jingliang Li,[*b] Linpeng Fan[b] and Xungai Wang[*a,b]

Received 00th January 20xx,
Accepted 00th January 20xx

DOI: 10.1039/x0xx00000x

www.rsc.org/

Uniform silver submicrospheres were synthesized under an ambient condition, through reduction of silver nitrate using ascorbic acid as a reducing agent and Tween 20 as a stabilizer. The silver submicroparticles exhibited strong catalytic activity for the reduction of 4-nitrophenol by sodium borohydride (NaBH4). Significantly, the aggregates of a few silver submicroparticles can be used as surface-enhanced Raman scattering (SERS) substrate to improve markedly the Raman signal of crystal violet. The morphologies of silver submicroparticles can be controlled by changing reaction conditions. The formation process of silver submicroparticles was monitored by time-resolved extinction spectroscopy. The influences of concentrations and molar ratios of reaction reagents on the formation of silver submicroparticles are discussed.

## 1. Introduction

Silver micro/nano materials have been widely explored for applications in many fields including surface enhanced spectroscopy, optoelectronics, catalysis, and biomedicine.[1-5] The intrinsic optical and electric properties of silver micro/nano materials are related to their size, shape, composition, and structure.[6, 7] A number of strategies have been attempted to prepare silver micro/nano particles, such as photoinduction [8, 9], thermal treatment,[10, 11] and sonochemical treatment.[12] Silver micro/nano particles were generally synthesized through reduction of silver nitrate ($AgNO_3$) in aqueous solutions by reductants such as citrate,[13] ascorbic acid,[14, 15] or borohydride.[16] Among these methods, reduction of silver ions with ascorbic acid, a mild reducing agent, is convenient and easy to control. Moreover, ascorbic acid is an eco-friendly and non-toxic substance. Fukuyo and Imai reduced $AgNO_3$ with ascorbic acid to obtain silver nanoparticles with unusual morphologies.[15] They suggested that flower-like particles were formed by outgrowth of petals around a seed and the ratio of ascorbic acid to $AgNO_3$ governed the morphology of the silver nanoparticles. Similarly, Wang et al synthesized coral-like silver particles by reducing $AgNO_3$ with ascorbic acid.[14] They proposed that the silver branches grew from a bulbous seed and formed aggregation. Concentrations and molar ratio of reagents ($AgNO_3$ and ascorbic acid) were found to determine the formation of branched structures. The role of stabilizer or surfactant in the synthesis of silver nanoparticles with ascorbic acid was also investigated.[14, 17-19] Polyvinylpyrrolidone (PVP) was demonstrated to inhibit the production of branched silver structures due to the strong capping and stabilizing effect of PVP.[14] Lou and co-workers synthesized hyperbranched silver nanocrystals with two-dimensional and gear-like structures and three-dimensional objects using $AgNO_3$ and ascorbic acid in the presence of trisodium citrate. They proposed that citrate and ascorbic acid played complementary roles in the formation of hyperbranched silver nanocrystals. Additives were observed to affect the morphologies of particles during reduction reaction of silver ions.

Tween 20 (polyoxyethylenesorbitan monolaurate) is one of non-ionic surfactants that have attracted attention recently in surface modification of noble metal nanoparticles, including silver and gold nanoparticles.[20-22] For example, Fathi and Kraatz demonstrated that Tween 20 could protect silver surface against corrosion in alkaline solution and lead to spherical non-packed nanoscaled silver surface.[23] In addition to its use in synthesis of nanoparticles, Tween 20 has also been used in surface functionalization of nanoparticles.[20, 24-27] For example, it was used to modify silver nanoparticles for detecting trace mercury ions in aqueous solutions through the amalgamation and aggregation of silver nanoparticles.[27] However, this surfactant has not been used for controlled synthesis of silver particles.

Silver particles at sub-micrometre scale have a variety of potential applications, such as catalysis,[6] electrically conductive paste,[19] photonic crystals,[28] sensing,[29] and surface-enhanced Raman scattering (SERS).[30] Size, shape and surface topography of submicron silver particles can significantly influence their optical, electric and surface properties, which are important for their applications.[31-33] For example, rough surfaces of silver particles can enhance the signal strength in SERS.[7, 31, 33] Therefore, it is significant to develop a facile, low-cost and environmentally friendly method to fabricate submicron silver particles as well as to explore their properties.

[a] School of Textile Science and Engineering, Wuhan Textile University, Wuhan 430073, China.
[b] Institute for Frontier Materials, Deakin University, Geelong, Victoria 3216, Australia.
*Corresponding author. E-mail: xungai.wang@deakin.edu.au; jingliang.li@deakin.edu.au.

Herein, a simple and green method was developed to prepare silver submicrospheres through reduction of silver ions with ascorbic acid in the presence of Tween 20. The influences of concentration and ratio of reaction reagents on the surface feature of silver submicroparticles were investigated. The catalytic property of as-synthesized silver submicroparticles was studied through monitoring reduction of 4-nitrophenol (4-NP) by sodium borohydride. Moreover, strong SERS effect was obtained on individual submicroparticles or the aggregates of silver submicroparticles including dimer and trimer.

## 2. Experimental section

### 2.1. Materials

$AgNO_3$ (>99%), L-Acetic acid (≥99.0%), Tween 20 (polyoxyethylenesorbitan monolaurate), Tween 80 (polyethylene glycol sorbitan monooleate), Triton X-100 (polyethylene glycol tert-octylphenyl ether), Tergitol (Type 15-S-7, secondary alcohol ethoxylate), crystal violet (Hexamethylpararosaniline chloride) (dye content ≥90.0%), 4-nitrophenol (≥99%) and sodium borohydride (>98%) were purchased from Sigma-Aldrich. All the chemicals were analytical grade and used as received.

### 2.2 Characterization

Scanning electron microscopy (SEM) measurements were performed with a Supra 55 VP field emission SEM. X-ray photoelectron spectroscopy (XPS) measurements were carried out on a Kratos XSAM800 XPS system with Kα source and a charge neutralizer. X-ray diffraction (XRD) patterns were collected using a Bruker D8 Advance X-ray diffractometer with Cu Kα radiation. Time-resolved ultraviolet-visible (UV-vis) extinction/absorption spectra were obtained with an Ocean Optics USB4000 Spectrometer and recorded using Ocean Optics SpectraSuite software.

### 2.3 Preparation of silver submicroparticles

$AgNO_3$ in Tween 20 aqueous solution was reduced to form silver submicroparticles by ascorbic acid at room temperature. An aqueous ascorbic acid solution (2 mL, different concentrations) was rapidly injected into 5 mL of aqueous solution containing $AgNO_3$ and Tween 20 under vigorous stirring. The final concentrations of Tween 20, $AgNO_3$ and ascorbic acid in mixed solutions were listed in Table 1. The reaction solutions turned gray within 30 s.

### 2.4 Catalytic activity

To investigate the catalytic efficiency of as-synthesized silver submicroparticles, the catalytic conversion of 4-nitrophenol (4-NP) into 4-aminophenol (4-AP) by sodium borohydride ($NaBH_4$) was performed in the presence of different silver submicroparticles. The samples (A1-E1) were centrifuged for 5 min at 10000 rpm to remove residual ascorbic acid and Tween 20 in solution. And then, the precipitated submicroparticles were redispersed in the same volume of deionised water for catalysis tests. In a typical experiment, 2.0 mL of 4-NP aqueous solution ($5.0 \times 10^{-5}$ M) was put into a quartz cuvette with a path length of 1 cm. 50 μL of silver submicroparticle solution was mixed with the 4-NP solution under stirring. Subsequently, 50 μL of $NaBH_4$ solution (1.0 M) was added to the mixed solution of 4-NP and silver submicroparticles under stirring. Meanwhile, time-resolved UV-vis absorption spectra were recorded. The parameters of time-resolved UV-vis absorption spectra were set as follows: integration time, 8 ms; scans to average, 10; boxcar width, 10; and interval, 10 s.

**Table 1.** Reaction conditions for synthesis of silver submicroparticles.

| [Tween 20] | [$AgNO_3$] | | | [Ascorbic acid] |
|---|---|---|---|---|
| | $3.6 \times 10^{-3}$ M | $1.8 \times 10^{-3}$ M | $3.6 \times 10^{-4}$ M | |
| $2.14 \times 10^{-4}$ M | A1 | A2 | A3 | $2.86 \times 10^{-2}$ M |
| $4.29 \times 10^{-4}$ M | B1 | B2 | B3 | $1.43 \times 10^{-2}$ M |
| $4.29 \times 10^{-4}$ M | C1 | C2 | C3 | $2.86 \times 10^{-2}$ M |
| $4.29 \times 10^{-4}$ M | D1 | D2 | D3 | $5.71 \times 10^{-2}$ M |
| $8.57 \times 10^{-4}$ M | E1 | E2 | E3 | $2.86 \times 10^{-2}$ M |

### 2.5 Spectral monitoring of formation process of silver submicroparticles

Time-resolved extinction spectroscopy was used to explore the rapid formation process of silver submicroparticles. In a typical implementation process, 1 mL of mixed solution of $AgNO_3$ and Tween 20 was put in a quartz cuvette with a path length of 1 cm. Then 0.40 mL of aqueous ascorbic solution was added into this mixed solution under vigorous stirring. The parameters of time-resolved UV-vis extinction spectra were set as follows: integration time, 8 ms; scans to average, 5; boxcar width, 10; and interval, 40 ms.

### 2.6 SERS measurement of crystal violet on silver submicroparticles

1.5 mL of as-prepared silver submicroparticles was centrifuged for 5 min at 10000 rpm. The supernatant was discarded and 1.5 mL of crystal violet ($10^{-7}$ M) aqueous solution was added in the centrifuge tube to disperse the precipitate of silver submicroparticles. After 2 h of incubation, the mixed solution was dropped on glass slides and dried under ambient condition for SERS measurement. SERS analysis was performed on a Renishaw inVia Raman microscope system (Renishaw plc, Wotton-under-Edge, UK). A 100 × /N.A. 0.90 objective and a 514-nm $Ar^+$ laser excitation source (50 mW, 5%) were used in all measurements. The spectra within a Raman shift window between 400 and 1700 $cm^{-1}$ were recorded using a mounted CCD camera with integration time of 5 s by a single scan.

## 3. Results and discussion

Fig. 1 shows the SEM images of silver particles synthesized under different conditions. The particles in SEM images of Sample A1 corresponding to $2.14 \times 10^{-4}$ M of Tween 20, $3.6 \times 10^{-3}$ M of $AgNO_3$ and $2.86 \times 10^{-2}$ M of ascorbic acid are in a "meatball" shape and with a diameter 537.6 ± 26.6 nm. It can be seen that the silver particles have an excellent monodispersity. The morphology of silver spheres did not change obviously when the concentration of silver ions was decreased from $3.6 \times 10^{-3}$ M to $1.8 \times 10^{-4}$ M (A1-A2 in Fig. 1). In

addition, the size and shape of silver particles corresponding to $3.6 \times 10^{-3}$ M and $1.8 \times 10^{-3}$ M of silver ions did not vary visibly as the concentration of Tween 20 was increased from $2.14 \times 10^{-4}$ M to $8.57 \times 10^{-4}$ M (A1-C1-E1 and A2-C2-E2 in Fig. 1). Nevertheless, the morphologies of silver particles changed with an increase in Tween 20 concentration when the silver particles were $3.6 \times 10^{-4}$ M (A3-C3-E3 in Fig. 1). Silver submicroparticles with a "Walnut" shape were obtained when the concentration of Tween 20 was increased to $8.57 \times 10^{-4}$ M (E3 in Fig. 1). The silver particles possess hollow structures, which can be seen from SEM images of the broken particles (A1, C1 and E1 in Fig. 1). The formation process of silver submicroparticles is suggested to include two stages: formation of silver nanoparticles and aggregation of silver nanoparticles to fabricate submicroparticles. In the first stage, the silver ions were reduced to silver atoms by ascorbic acid and formed silver nanoparticles through nucleation process. It was reported that silver flowers were obtained if the reaction contained only ascorbic acid and $AgNO_3$ without surfactants.[14, 15] In the present study, uniform silver submicroparticles were fabricated, which may be due to the stabilizing and directing effects of Tween 20. In the second stage, the silver nanoparticles formed in the first stage then aggregated with assistance of Tween 20 to fabricate lager silver particles. The quantity of formed silver nanoparticles was small when the silver ion concentration was low ($3.6 \times 10^{-4}$ M). Consequently, Tween 20 could effectively coat the surface of silver nanoparticles and prevent their aggregation, which resulted in "walnut" silver particles (E3 in Fig. 1). A high resolution SEM image shows that the as-synthesized silver particles are composed of many nanoparticles (Fig. 2A). The silver submicroparticles are very uniform as observed from the SEM image at a low magnification (Fig. 2B), which further proves the excellent monodispersity of the particles.

Moreover, silver ions were reduced by ascorbic acid in the absence of Tween 20 to investigate the effect of tween 20. Fig. S1 shows the SEM images of silver particles obtained from different concentrations of silver ions ($3.6 \times 10^{-3}$ M, $1.8 \times 10^{-3}$ M and $3.6 \times 10^{-4}$ M) without Tween 20. A few silver submicroparticles can be observed in the SEM images. However, most of particles were not regular and they aggregated together at all the silver ion concentrations (Fig. S1). The results clearly verify that Tween 20 played a critical role in assisting fabrication of submicroparticles from small nanoparticles. Other non-ionic surfactants including Tween 80, Triton X-100 and Tergitol 15-S-7 were used instead of Tween 20 to inspect the effect of non-ionic surfactants in synthesis of silver submicroparticles. Fig. S2 and S3 display the SEM images of silver particles in the different non-ionic surfactants. As can be seen, the spherical silver submicroparticles were obtained with assistance of Tween 80, Triton X-100 and Tergitol 15-S-7, which indicates that non-ionic surfactants exhibit similar property to prevent the aggregation of silver nanoparticles and assist the formation of silver submicroparticles.

To gain insights into the influence of ascorbic acid on the morphologies of silver particles, different concentrations of ascorbic acid were used. Fig. 3 shows SEM images of silver

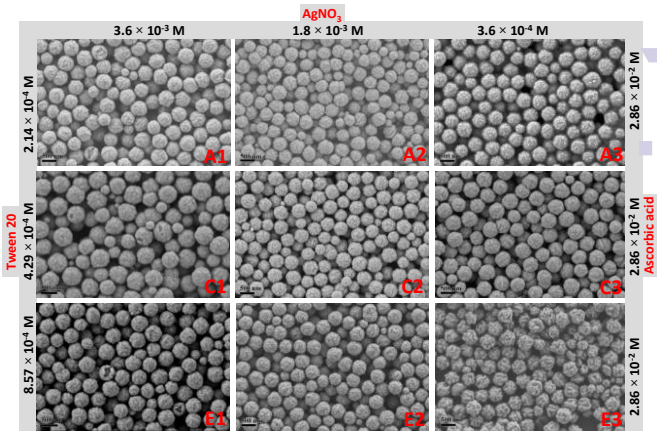


Fig. 1 SEM images of silver particles obtained under different reaction conditions corresponding to Table 1. The scale bars represent 500 nm.

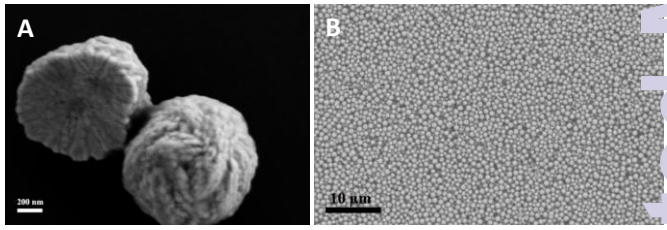


Fig. 2 SEM images of silver submicroparticles at (A) high and (B) low magnification.

submicroparticles obtained at ascorbic acid concentrations of $1.43 \times 10^{-2}$ M and $5.71 \times 10^{-2}$ M. Comparing the SEM images from different concentration of ascorbic acid (Images B1-B3, C1-C3 and D1-D3 in Fig. 1 and 3), uniformity of particles decreased as the concentration of ascorbic acid was lowered. The shape of silver nanoparticles are not regular (B1 in Fig. 3), which indicates that ascorbic acid plays an important role in the aggregation of silver nanoparticles. Interestingly, silver nanoflowers were obtained when the silver ion concentration decreased to $3.6 \times 10^{-4}$ M at the ascorbic concentration of $1.43 \times 10^{-2}$ M. Increasing ascorbic acid favoured the formation of regular silver particles (D1-D3 in Fig. 3). The results reveal that ascorbic acid has significant influence on the morphologies of silver nanoparticles. The sizes of silver submicroparticles obtained under different conditions were measured using SEM images and the results are given in Table 2. The average diameters of the most silver particles are in the range of 400 ~ 500 nm.

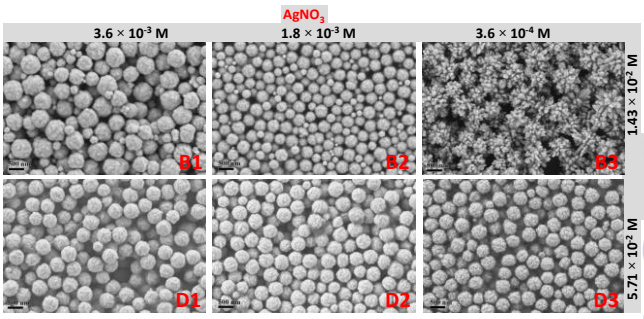


Fig. 3 SEM images of silver particles corresponding to Table 1. The concentration of Tween 20 was fixed at $4.29 \times 10^{-2}$ M. The scale bars represent 500 nm.

Table 2 Diameters of silver particles under different conditions.

| ID | Size (nm) | ID | Size (nm) | ID | Size (nm) | ID | Size (nm) | ID | Size (nm) |
|---|---|---|---|---|---|---|---|---|---|
| A1 | 537.6±26.6 | B1 | 539.1±87.2 | C1 | 550.8±82.0 | D1 | 493.2±42.6 | E1 | 500.7±32.7 |
| A2 | 421.3±32.6 | B2 | 389.3±35.6 | C2 | 482.8±54.3 | D2 | 459.4±33.2 | E2 | 507.7±32.1 |
| A3 | 500.4±31.1 | B3 | / | C3 | 533.1±29.9 | D3 | 425.6±36.9 | E3 | 467.6±34.3 |

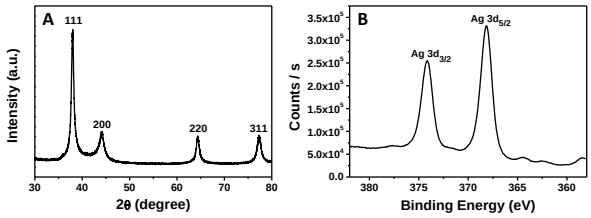


Fig. 4 (A) XRD pattern and (B) XPS spectrum of the synthesized silver submicroparticles (Sample C2).

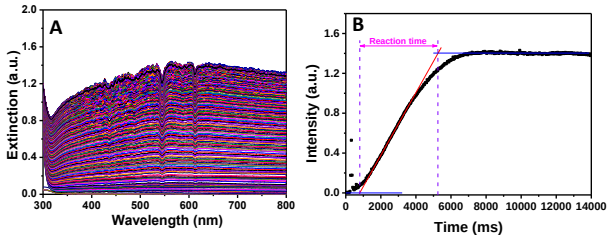


Fig. 5 (A) Time-resolved extinction spectra of reaction solution (Sample C2) and (B) plot of corresponding extinction intensity at 600 nm as a function of reaction time. The interval time between extinction spectra was 40 ms.

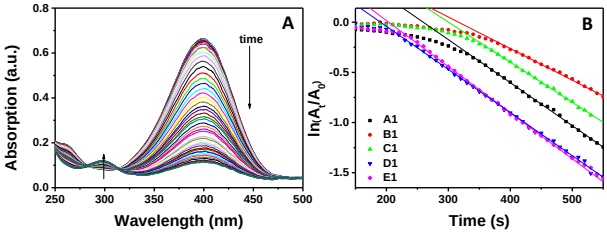


Fig. 6 Evolution of UV-vis absorption spectra of 4-nitrophenol solution with silver submicroparticles (Sample E1) after $NaBH_4$ solution was added. (B) Plots of $\ln(A_t/A_0)$ of the absorption peak for 4-NP (400 nm) as a function of time in the presence of different silver submicroparticles.

To examine the crystal structure and phase purity of the as-prepared silver particles, XRD characterization was performed, as shown in Fig. 4A. In the XRD curve, four narrow reflection peaks appeared at 38°, 44°, 64° and 77°, which are assigned to the (111), (200), (220), and (311) crystalline planes of a face centered cubic (fcc) structure of silver, respectively.[33] The high and sharp XRD peaks indicate that the as-synthesized silver particles are well crystallized. No impurity phase was detected in the sample. To further verify the formation of silver atoms from $AgNO_3$, XPS characterization was performed. The Ag 3d XPS region of the silver particles is depicted in Fig. 4B. Two peaks centered at of 374.2 eV and 368.2 appeared in XPS curve, which are attributed to Ag $3d_{3/2}$ and Ag $3d_{5/2}$, respectively. The binding energy values of XPS peaks are in agreement with metallic silver, demonstrating the formation of metallic silver.[29, 34]

The formation of silver submicroparticles is very fast (less than 30 s). Fig. 5A displays time-resolved extinction spectra of a reaction solution with ascorbic acid (0.40 mL, 0.10 M) added into a solution (1.00 mL) containing $AgNO_3$ ($1.8 \times 10^{-3}$ M) and Tween 20 ($4.29 \times 10^{-4}$ M). As can be seen, a broad extinction band appeared in the region with wavelengths longer than 350 nm, indicating silver particles with wide morphologies were produced. The intensity of whole spectra at wavelengths longer than 350 nm increased as reaction time was prolonged, which may be due to the formation of silver submicroparticles from aggregation of silver nanoparticles. To investigate the rate of formation of silver submicroparticles, the intensity at 600 nm was plotted as a function of reaction time (Fig. 5B). The reaction time could be calculated using the plots of intensity *vs* time. The reaction times corresponding to Samples C1-C3 were 4546 ± 65 ms, 5460 ± 281 and 6390 ± 171 ms, respectively, indicating that the formation of silver submicroparticles was very fast. The reaction time decreased with a decrease in silver ion concentration from Sample C1 ($3.6 \times 10^{-3}$ M) to Sample C3 ($3.6 \times 10^{-4}$ M). The reaction times for Samples B2 and D2 were 4739 ± 494 ms and 6199 ± 199 ms, respectively. When the concentrations of silver ions and Tween 20 were fixed, increasing ascorbic acid concentration sped the formation of silver submicroparticles.

The reduction of 4-nitrophenol (4-NP) have become a common catalytic model reaction to test the catalytic activity of metal particles in aqueous solution.[35] The catalytic activity of the as-prepared silver submicroparticles were evaluated through monitoring UV-vis absorption spectra of aqueous solution during the reduction of 4-nitrophenol (4-NP) by sodium borohydride ($NaBH_4$). The solution of 4-NP presented an absorption peak at 400 nm after adding NaBH4 solution, which is assigned to 4-nitrophenolate ions.[36] Fig. 6A show time-resolved UV-vis absorption spectra of solutions containing 4-nitrophenol and $NaBH_4$ in the presence silver submicroparticles (Sample E2). After adding $NaBH_4$, the intensity of the absorption peak of 4-NP at 400 nm decreased as time was prolonged (Fig. 6A). In the meantime, a new absorption peak at 300 nm appeared during this process, which implies the formation of 4-aminophenol (4-AP).[37, 38] The reduction rate of 4-NP can be indicated by the intensity change of absorption peak at 400 nm. Fig. S4 plots the absorption peak intensity at 400 nm as a function of time corresponding to different silver submicroparticles (A1-E1). The absorption intensity at 400 nm of 4-nitrophenol solution with silver submicroparticles changed dramatically, revealing that the silver submicroparticles have remarkable catalytic activity for reduction of 4-nitrophenol by $NaBH_4$. In the presence of excess $NaBH_4$, the reduction of 4-NP is generally treated as pseudo-first-order kinetic reaction.[39, 40] Fig. 6B shows the plots of $\ln(A_t/A_0)$ versus time. $A_t$ represents the absorption at 400 nm at the time of *t*, and $A_0$ represents the absorption at the initial stage. The value of $\ln(A_t/A_0)$ was

constant at the beginning of the reaction and then decreased linearly after certain time. The constant of peak intensity at 400 nm remained constant for certain time before decreasing suggests the presence of an induction time for reduction reaction of 4-NP [41] The linear correlation between $\ln(A_t/A_0)$ and time as seen from Fig. 6B supports the pseudo-first-order assumption. The apparent rate constant ($K_{app}$) of the catalytic reactions can be obtained from the linear slop of $\ln(A_t/A_0)$ versus time.[40, 42, 43] The $K_{app}$ values of reduction reaction in the presence of Samples A1-E1 were estimated to be $4.28 \times 10^{-3}$, $3.15 \times 10^{-3}$, $4.00 \times 10^{-3}$, $4.31 \times 10^{-3}$ and $4.60 \times 10^{-3}$ $S^{-1}$, respectively. The $K_{app}$ values obtained in this study are compared to the related results in literature for silver particles.[6, 40, 44-47] For example, Jiang and co-workers reported that the kinetic reaction rate of catalytic reaction with synthesized submicron-sized silver particles was $2.15 \times 10^{-3}$ $S^{-1}$.[6] The highest reaction constant obtained by Cai et al. was $2.3 \times 10^{-3}$ $S^{-1}$.[40] Although the $K_{app}$ values of catalytic reduction from the present silver submicroparticles are slightly smaller than those from the nano-sized silver particles,[36, 43] the facile synthesis and easy separation of the silver submicroparticles obtained in this research conduce to their application in catalytic reactions.

The silver submicroparticles were separated from an original aqueous solution and redispersed in water. As shown in Fig. 7A, some silver submicroparticles aggregate to form dimers, trimers and multimers after the redispersed solutions were dropped on glass slide and dried. It is well known that silver micro/nano structures can serve as active substrates to enhance Raman signal. In this study, the SERS activity of silver submicroparticles was evaluated using crystal violet (CV) as a probe. The SERS spectra were collected from one of the bright spots in the dark-field optical image of silver submicroparticles (Fig. 7B). The synthesized submicroparticles could enhance significantly the Raman signal of CV. Fig. 8A and B show the SERS spectra of $10^{-7}$ M of CV from individual submicroparticles or aggregates of a few submicroparticles (dimers, trimers, etc) (Samples A1 and B1). Strong Raman peaks were obtained through surface-enhancement effect of silver submicroparticles even when the concentration of CV is as low as $10^{-7}$ M. Compared with the normal Raman spectrum of $10^{-4}$ M CV (Curve a in Fig. 8C), the Raman peaks of $10^{-7}$ M from silver submicroparticles were notably high, implying silver submicroparticles possess strong SERS activity. In addition, the Raman spectrum of submicroparticles (Sample A1) did not exhibit distinct characteristic Raman bands of CV (Curve b in Fig. 8C). Extremely strong SERS signal of probe molecule from single submicroparticles or aggregates of a few silver submicroparticles demonstrate that the synthesized silver submicroparticles have excellent SERS activity that can be used as SERS substrates for detecting trace analytes.

## 4. Conclusions

A simple morphology controlled synthesis approach of silver submicroparticles was developed using $AgNO_3$, ascorbic acid and Tween 20. The prepared silver particles were "meatball" or

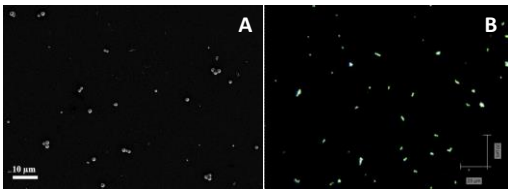


Fig. 7 (A) SEM image and (B) dark-field optical images of silver submicroparticles redispersed in water.

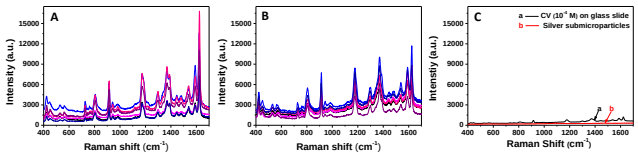


Fig. 8 SERS spectra of crystal violet (CV) of $10^{-7}$ M from aggregates of submicroparticles redispersed in CV aqueous solution ($10^{-7}$ M): (A) Sample A1 and (B) Sample B1. (C) Raman spectra of Sample A1 without CV and pure CV ($10^{-4}$ M CV dropped on glass to dry).

"walnut" submicrospheres. The uniformity of silver submicrospheres was excellent, which may favour the fabrication of photonic crystals. The influences of concentration and molar ratio of reaction reagents on the size and morphology of silver particles were investigated. The synthesis of silver submicroparticles was proposed to include formation and aggregation of silver nanoparticles. As characterized with time-resolved absorption spectroscopy, the formation of silver submicroparticles was very fast (within 30 s). The obtained silver particles have significant catalytic activity. The single submicroparticles or aggregates of a few silver submicrospheres show strong surface-enhanced Raman scattering (SERS) effect, which can be used for detection of trace analytes.

## Acknowledgements

This research was supported by the National Natural Science Foundation of China (NSFC 51273153 and 51403162).

## Notes and references

1. S.-H. Cao, W.-P. Cai, Q. Liu, K.-X. Xie, Y.-H. Weng, S.-X. Huo, Z.-Q. Tian and Y.-Q. Li, *J. Am. Chem. Soc.,* 2014, **136**, 6802-6805.
2. J. A. Scholl, A. L. Koh and J. A. Dionne, *Nature*, 2012, **483**, 421-U468.
3. J. Henzie, M. Gruenwald, A. Widmer-Cooper, P. L. Geissler and P. Yang, *Nat. Mater.,* 2012, **11**, 131-137.
4. L. Yang, P. Li, H. Liu, X. Tang and J. Liu, *Chem. Soc. Rev.,* 2015, **44**, 2837-2848.
5. H. Wang, Y. Zhou, X. Jiang, B. Sun, Y. Zhu, H. Wang, Y. Su and Y. He, *Angew. Chem.-Int. Edit.*, 2015, **54**, 5132-5136.
6. D. Jiang, J. Xie, M. Chen, D. Li, J. Zhu and H. Qin, *J. Alloys Compd.,* 2011, **509**, 1975-1979.
7. L. Lu, A. Kobayashi, K. Tawa and Y. Ozaki, *Chem. Mat.*, 2006, **18**, 4894-4901.
8. B. Tang, L. Sun, J. L. Li, M. W. Zhang and X. A. Wang, *Chem. Eng. J.,* 2015, **260**, 99-106.
9. R. Jin, Y. Cao, C. A. Mirkin, K. L. Kelly, G. C. Schatz and J. G. Zheng, *Science*, 2001, **294**, 1901-1903.
10. Y. Sun, B. Mayers and Y. Xia, *Nano Lett.,* 2003, **3**, 675-679.

11. Q. B. Zhang, J. P. Xie, J. H. Yang and J. Y. Lee, *Acs Nano*, 2009, **3**, 139-148.
12. H. Xu and K. S. Suslick, *ACS Nano*, 2010, **4**, 3209-3214.
13. Z. S. Pillai and P. V. Kamat, *J. Phys. Chem. B*, 2004, **108**, 945-951.
14. Y. Wang, P. H. C. Camargo, S. E. Skrabalak, H. Gu and Y. Xia, *Langmuir*, 2008, **24**, 12042-12046.
15. T. Fukuyo and H. Imai, *J. Cryst. Growth* 2002, **241**, 193-199.
16. G. Wei, H. L. Zhou, Z. G. Liu, Y. H. Song, L. Wang, L. L. Sun and Z. Li, *J. Phys. Chem. B*, 2005, **109**, 8738-8743.
17. Z. Liu, X. Qi and H. Wang, *Adv. Powder Technol.,* 2012, **23**, 250-255.
18. J. H. Yang, L. M. Qi, D. B. Zhang, J. M. Ma and H. M. Cheng, *Cryst. Growth Des.*, 2004, **4**, 1371-1375.
19. R. Irizarry, L. Burwell and M. S. Leon-Velazquez, *Ind. Eng. Chem. Res.*, 2011, **50**, 8023-8033.
20. C.-Y. Lin, C.-J. Yu, Y.-H. Lin and W.-L. Tseng, *Anal. Chem.*, 2010, **82**, 6830-6837.
21. M. Harada, Y. Kimura, K. Saijo, T. Ogawa and S. Isoda, *J. Colloid Interface Sci.,* 2009, **339**, 373-381.
22. M. R. Hormozi-Nezhad, P. Karami and H. Robatjazi, *Rsc Advances*, 2013, **3**, 7726-7732.
23. F. Fathi and H.-B. Kraatz, *Analyst*, 2013, **138**, 5920-5925.
24. T. Lou, Z. Chen, Y. Wang and L. Chen, *ACS Appl. Mat. Interfaces* 2011, **3**, 1568-1573.
25. X. Wang, Y. Wei, S. Wang and L. Chen, *Colloid. Surface. A*, 2015, **472**, 57-62.
26. N. Bi, Y. Chen, H. Qi, X. Zheng, Y. Chen, X. Liao, H. Zhang and Y. Tian, *Spectroc Acta Pt. A-Molec. Biomolec. Spectr.*, 2012, **95**, 276-281.
27. L. Zhuang, C. Zheng, J. Sun, A. Yuan and G. Wang, *Fibers Polym.,* 2014, **15**, 226-233.
28. J. F. Galisteo-Lopez, M. Ibisate, R. Sapienza, L. S. Froufe-Perez, A. Blanco and C. Lopez, *Adv. Mater.,* 2011, **23**, 30-69.
29. X. Fan, Z.-W. Liu, J. Lu and Z.-T. Liu, *Ind. Eng. Chem. Res.*, 2009, **48**, 6212-6215.
30. D.-P. Yang, S. Chen, P. Huang, X. Wang, W. Jiang, O. Pandoli and D. Cui, *Green Chem.*, 2010, **12**, 2038-2042.
31. F. De Angelis, F. Gentile, F. Mecarini, G. Das, M. Moretti, P. Candeloro, M. L. Coluccio, G. Cojoc, A. Accardo, C. Liberale, R. P. Zaccaria, G. Perozziello, L. Tirinato, A. Toma, G. Cuda, R. Cingolani and E. Di Fabrizio, *Nat. Photonics* 2011, **5**, 683-688.
32. W. L. Barnes, A. Dereux and T. W. Ebbesen, *Nature*, 2003, **424**, 824-830.
33. C.-Y. Chen and C.-P. Wong, *Nanoscale*, 2014, **6**, 811-816.
34. X. P. Sun, S. J. Dong and E. K. Wang, *J. Colloid Interface Sci.,* 2005, **290**, 130-133.
35. P. Herves, M. Perez-Lorenzo, L. M. Liz-Marzan, J. Dzubiella, Y. Lu and M. Ballauff, *Chem. Soc. Rev.,* 2012, **41**, 5577-5587.
36. N. Muthuchamy, A. Gopalan and K.-P. Lee, *RSC Adv.*, 2015, **5**, 76170-76181.
37. J. E. Cloud, L. W. Taylor and Y. A. Yang, *RSC Adv.*, 2014, **4**, 24551-24559.
38. M. Liang, R. X. Su, R. L. Huang, W. Qi, Y. J. Yu, L. B. Wang and Z. M. He, *ACS Appl. Mat. Interfaces* 2014, **6**, 4638-4649.
39. M. M. Nigra, J.-M. Ha and A. Katz, *Catal. Sci. Technol.*, 2013, **3**, 2976-2983.
40. Y. K. Cai, K. L. Gao, G. C. Li, Z. J. Deng and G. Z. Han, *Colloid. Surface. A*, 2015, **481**, 407-412.
41. M. A. Mahmoud and M. A. El-Sayed, *Nano Lett.,* 2011, **11**, 946-953.
42. S. Wunder, F. Polzer, Y. Lu, Y. Mei and M. Ballauff, *The J. Phys. Chem. C*, 2010, **114**, 8814-8820.
43. Y. Mao, J. Wei, C. Wang, Y. Feng, H. Yang and X. Meng, *Mater. Lett.,* 2015, **154**, 47-50.
44. M. H. Rashid and T. K. Mandal, *J. Phys. Chem. C* 2007, **111**, 16750-16760.
45. S. Tang, S. Vongehr and X. Meng, *J. Phys. Chem. C*, 2010, **114**, 977-982.
46. X. Li, J. Wang, Y. Zhang, M. Li and J. Liu, *Eur. J. Inorg. Chem.*, 2010, **2010**, 1806-1812.
47. L. Ai, H. Yue and J. Jiang, *J. Mater. Chem.,* 2012, **22**, 23447-23453.

## Graphical Abstract

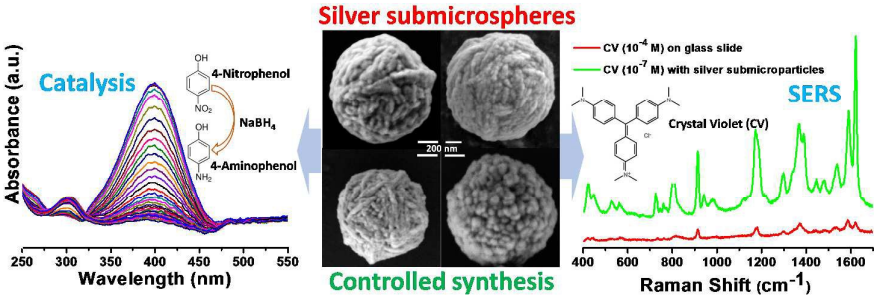


Silver submicrospheres fabricated under an ambient condition can catalyze the reduction of 4-nitrophenol and improve significantly the Raman signal of crystal violet as surface-enhanced Raman scattering (SERS) substrate.